Available online at www.sciencedirect.com
ScienceDirect
Comput. Methods Appl. Mech. Engrg. 283 (2015) 503–516
Computer methods in applied mechanics and engineering
www.elsevier.com/locate/cma

Topology optimization for microstructures of viscoelastic composite materials

Xiaodong Huang[a,b,*], Shiwei Zhou[b], Guangyong Sun[a], Guangyao Li[a], Yi Min Xie[b]

[a] State Key Laboratory of Advanced Design and Manufacturing for Vehicle Body, Hunan University, Changsha, Hunan, 410082, PR China
[b] Centre for Innovative Structures and Materials, School of Civil, Environmental and Chemical Engineering, RMIT University, GPO Box 2476, Melbourne 3001, Australia

Received 1 July 2014; received in revised form 2 October 2014; accepted 8 October 2014
Available online 16 October 2014

Highlights

- An extended BESO method for designing microstructures of viscoelastic composites.
- Unambiguous microstructures of viscoelastic composites are obtained.
- Composites with desirable viscoelastic properties are presented.
- Comparison with theoretical bounds of storage and loss moduli.

Abstract

The viscoelastic response of materials is often utilized for wide applications such as vibration reduction devices. This paper extends the bi-directional evolutionary structural optimization (BESO) method to the design of composite microstructure with optimal viscoelastic characteristics. Both storage and loss moduli of composite materials are calculated through the homogenization theory using complex variables. Then, the BESO method is established based on the sensitivity analysis. Through iteratively redistributing the base material phases within the unit cell, optimized microstructures of composites with the desirable viscoelastic properties will be achieved. Numerical examples demonstrate the effectiveness of the proposed optimization method for the design of viscoelastic composite materials. Various microstructures of optimized composites are presented and discussed. Meanwhile, the storage and loss moduli of the optimized viscoelastic composites are compared with available theoretical bounds.

Keywords: Topology optimization; Viscoelastic composite; Microstructure; Bi-directional evolutionary structural optimization (BESO)

* Corresponding author at: Centre for Innovative Structures and Materials, School of Civil, Environmental and Chemical Engineering, RMIT University, GPO Box 2476, Melbourne 3001, Australia. Tel.: +61 3 99253320; fax: +61 3 96390138.
E-mail address: huang.xiaodong@rmit.edu.au (X. Huang).

http://dx.doi.org/10.1016/j.cma.2014.10.007
0045-7825/

1. Introduction

Vibration is often undesirable for structures due to the demands for structural stability, durability and noise reduction. Viscoelastic materials such as rubbers are often applied for reducing the vibration level through damping mechanisms [1,2]. Those viscoelastic materials have favorable damping characteristics but often lack stiffness for constructing engineering products. Composites may produce the high damping and high stiffness by mixing two or more constituent materials with different physical properties [3]. The resulting viscoelastic composites will be of great interest to various industries such as automobile, aerospace, etc. The viscoelastic response of these artificial composites mainly depends on their microstructures apart from the proportion and physical properties of their constituents [1,3]. Designing viscoelastic composites with high damping and stiffness could be achieved by formulating a topology optimization problem for micro-structural topology and material properties at the macro scale.

Topology optimization methods, e.g. homogenization method [4], Solid Isotropic Material with Penalization (SIMP) [5–8], level set method [9–11], Evolutionary Structural Optimization (ESO) [12,13] and its later version Bi-directional ESO (BESO) [14,15], were originally developed to find a stiffest structural layout under given constraints. Topology optimization for the material design was initially proposed by Sigmund [16,17]. It was assumed that the material was microscopically composed of periodical unit cells (PUCs) and its effective macroscopic properties could be calculated through the homogenization theory. The inverse homogenization problem for seeking the best microstructure of the unit cell with the prescribed constitutive properties was then solved by topology optimization technique. Since then, extensive research has been carried out to investigate the material design with prescribed or extreme effective mechanical properties [18,19], thermal conductivity [20], permeability [21] and electromagnetic properties [22,23], the combination of properties [24–26], and so on.

Different from the pure elastic materials, viscoelastic materials have complex moduli, namely storage modulus and loss modulus. Early studies on viscoelastic composites focused on the bounds of effective complex moduli and found that multi-scale microstructures such as the Hashin–Shtrikman coated spheres assemblage or rank-N laminates could achieve high stiffness and high damping [27–30]. With the development of the modern manufacture technologies such as 3D printers, it is worthwhile to optimally design one-length scale microstructures with clear boundaries for viscoelastic composites. Topology optimization was firstly applied to the design of microstructures of viscoelastic composites for optimal damping characteristics by Yi et al. [31] and obtained the microstructures of viscoelastic composites. Prasad and Diaz [32] conducted the topology optimization of viscoelastic materials utilizing negative stiffness components. Recently, Chen and Liu [33] investigated topology optimization for the design of viscoelastic cellular materials with prescribed properties. Most recently, Andreasen et al. [34] investigated microstructures of viscoelastic composites which achieve the theoretical upper bound by topology optimization and Andreassen and Jensen [35] further studied viscoelastic composites for maximizing the loss/attenuation of propagating waves.

It has been revealed that optimized material microstructures highly depended on the used optimization parameters and algorithm because a number of different microstructures could possess the same physical property [16–19]. Because of the simplicity and computational efficiency of the BESO method [15,36,37], this paper will investigate the topology optimization of viscoelastic composites by using the BESO method with discrete design variables. Composite materials are assumed to be composed of two base materials (at least one is viscoelastic material) and their microstructures are uniformly represented by corresponding periodic unit cells. The optimization objective is to find the optimal distribution of two base materials within the unit cell so that the resulting composite has the maximum damping and/or stiffness. The homogenization theory will be used to calculate the effective properties of viscoelastic composites and then the BESO method will be applied for finding their optimal microstructures. Several numerical examples will be presented and compared with the theoretical bounds to demonstrate the effectiveness of the proposed BESO method.

2. Homogenization for viscoelastic composites

2.1. Properties of viscoelastic materials in the frequency domain

When a uniform viscoelastic material is subjected to a sinusoidally varying stress with the operation frequency, ω, the resulting strain also varies sinusoidally with the same frequency when a steady state is eventually reached. The

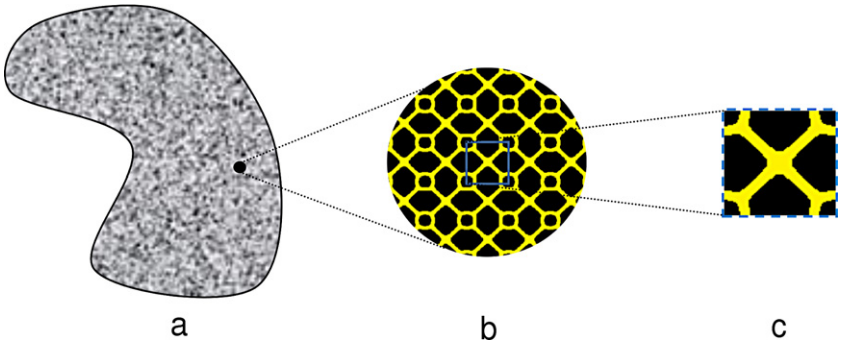

Fig. 1. (a) Macroscopic structure; (b) composite microstructure; (c) periodic unit cell.

stress and strain varying with time at the steady state are expressed by

$$\sigma_{ij}(\omega,\ t) = \bar{\sigma}_{ij}(\omega)\exp(i\omega t) \tag{1}$$

$$\varepsilon_{kl}(\omega,\ t) = \bar{\varepsilon}_{kl}(\omega)\exp(i\omega t) \tag{2}$$

where $\bar{\sigma}_{ij}$ and $\bar{\varepsilon}_{kl}$ are the spatial part of the stress and strain and their relationship is given by [2]

$$\bar{\sigma}_{ij}(\omega) = E_{ijkl}\,(\omega)\,\bar{\varepsilon}_{kl}(\omega) \tag{3}$$

where $E_{ijkl}(\omega)$ is the complex modulus which also depends on the operation frequency. The complex modulus $E_{ijkl}(\omega)$ in the frequency domain can be measured by the relaxation modulus in the time domain through the Fourier transform as

$$E_{ijkl}\,(\omega) = i\omega\int_0^\infty E_{ijkl}(t)\exp(-i\omega t)dt. \tag{4}$$

The complex modulus can be explicitly divided into the real and imaginary parts as

$$E_{ijkl}(\omega) = E'_{ijkl}\,(\omega) + iE''_{ijkl}(\omega) \tag{5}$$

where $E'_{ijkl}\,(\omega)$ is the storage modulus and $E''_{ijkl}(\omega)$ is the loss modulus. The loss tangent $\tan\delta_{ijkl}$ as a measure of damping is the ratio of the loss modulus to the storage modulus, which is proportional to the energy loss per cycle within the framework of linear viscoelasticity.

2.2. *Effective complex modulus of viscoelastic composites*

It is assumed that the macroscopic structure as shown in Fig. 1(a) is made by a composite which is composed of two-phase base materials where at least one material phase is viscoelastic. The microstructure of the composite as shown in Fig. 1(b) is spatially repeated with the periodic unit cell in Fig. 1(c). When the size of the periodic unit cell is quite small compared with the wavelengths of all relevant elastic waves, the macroscopic properties of the viscoelastic composite can be homogenized over the unit cell. At any given frequency, the homogenized relationship between the spatial parts of the stress and strain in the heterogeneous composite is then expressed by

$$\bar{\sigma}_{ij}(\omega) = E^H_{ijkl}\,(\omega)\,\bar{\varepsilon}_{kl}(\omega) \tag{6}$$

where $E^H_{ijkl}(\omega)$ is the effective complex modulus which depends on the properties of base materials, the volume fractions and spatial distribution of material phases in the unit cell. With the asymptotic approximations, the effective complex modulus can be obtained by the homogenization theory [38–40] as

$$E^H_{ijkl}(\omega) = \frac{1}{|Y|}\int_\Omega E_{ijpq}(\omega)(\bar{\varepsilon}^{kl}_{pq} - \tilde{\varepsilon}^{kl}_{pq})d\Omega \tag{7}$$

where $|Y|$ denotes the area (or volume in 3D) of the unit cell domain Ω. $\bar{\varepsilon}^{kl}_{pq}$ defines the four linearly independent unit strain fields as $\bar{\varepsilon}^{11}_{pq} = \begin{pmatrix}1 & 0 & 0 & 0\end{pmatrix}^{\mathrm{T}}$, $\bar{\varepsilon}^{22}_{pq} = \begin{pmatrix}0 & 1 & 0 & 0\end{pmatrix}^{\mathrm{T}}$, $\bar{\varepsilon}^{12}_{pq} = \begin{pmatrix}0 & 0 & 1 & 0\end{pmatrix}^{\mathrm{T}}$ and $\bar{\varepsilon}^{21}_{pq} = \begin{pmatrix}0 & 0 & 0 & 1\end{pmatrix}^{\mathrm{T}}$ for 2D cases.

The strain fields $\tilde{\varepsilon}^{kl}_{pq}$ induced by the test strains can be found from the following equation

$$\int_{\Omega} E_{ijpq}(\omega)\varepsilon_{ij}(v)\tilde{\varepsilon}^{kl}_{pq}d\Omega = \int_{\Omega} E_{ijpq}(\omega)\varepsilon_{ij}(v)\bar{\varepsilon}^{kl}_{pq}d\Omega \tag{8}$$

where $v \in H^1_{per}(\Omega)$ which is the Y-periodic admissible displacement field. The above equation is the weak form of the standard elasticity equation applied to the unit cell with periodic boundary conditions subject to the independent cases of pre-strain given by $\bar{\varepsilon}^{kl}_{pq}$.

The effective complex modulus, E^H_{ijkl} can be found by substituting the solution of Eq. (8), $\tilde{\varepsilon}^{kl}_{pq}$ into Eq. (7). It can be seen that the above homogenization expressions are the same to those for pure elastic materials except that the properties of the viscoelastic phase depends on the operation frequency. Furthermore, it should also note that both E_{ijpq} and $\tilde{\varepsilon}^{kl}_{pq}$ in the equations are complex and thus Eq. (8) will be solved by finite element analysis with complex variables in this paper.

3. Topology optimization

3.1. Design variables and material interpolation scheme

The effective stiffness and damping of a two-phase composite highly depend on the spatial distribution of material phases, therefore, how to optimally distribute material phases within the unit cell would be critical in the design of viscoelastic composites. In this paper, the unit cell is discretized into finite elements and each element is assigned with either material 1 or material 2. An artificial design variable, x_e, is introduced by assuming that $x_e = 1$ if an element is made of material 1 and $x_e = 0$ if an element is made of material 2. With such an assumption, Yi et al. [31] employed a linear artificial two-phase material model as

$$E_{ijkl}(x_i) = x_e E^{(1)}_{ijkl} + (1 - x_e)E^{(2)}_{ijkl} \tag{9}$$

where $E^{(1)}_{ijkl}$ and $E^{(2)}_{ijkl}$ are the moduli of material 1 and material 2 respectively. Due to lack of proper penalization scheme, the resulting solutions contained a large volume of "gray area" with intermediate design variables [31]. In the BESO method, we will use the binary design variable $x_e = 0$ or 1 only and the solutions will give clearly boundaries between material 1 and material 2. However, it should be noted that BESO can only find a convergent 0/1 solution when the solution exists [41,42]. In the solid isotropic material penalization (SIMP) method [5–8], the well-known SIMP model [5–8] makes elements with intermediate design variables density uneconomical in the optimization process and thus the solution naturally tends to be 0/1. However, our numerical tests indicated that the solutions are hardly convergent to 0/1 designs by directly employing the SIMP model for viscoelastic material design. Andreasen et al. [34] have investigated the influence from the penalization parameter for the complex modulus and suggested to use a power-law exponent less than 1 for the imaginary part. As a compromise no penalization is used for both real and imaginary moduli [34]. Here, we establish artificial two-phase material models for storage modulus and loss modulus separately. The storage modulus uses the SIMP model as

$$E'_{ijkl}(x_i) = x_e^p E'^{(1)}_{ijkl} + (1 - x_e^p)E'^{(2)}_{ijkl} \tag{10}$$

where $E'^{(1)}_{ijkl} > E'^{(2)}_{ijkl}$. p is the exponent of penalization and it has been verified that the optimization solution tends to 0/1 as $p > 1$ [8]. Therefore, $p = 3$ is used throughout this paper. Meanwhile, the linear relationship is defined for the loss modulus by

$$E''_{ijkl}(x_e) = x_e E''^{(1)}_{ijkl} + (1 - x_e)E''^{(2)}_{ijkl} \tag{11}$$

where $E''^{(1)}_{ijkl}$ and $E''^{(2)}_{ijkl}$ are the loss moduli of material 1 and material 2 respectively. Our numerical examples will demonstrate that the above material interpolation schemes work well for maximizing damping and/or stiffness of viscoelastic composites reported in this paper.

3.2. Statement of the optimization problem

The high stiffness and/or high damping at the operation frequency are desirable for the design of viscoelastic materials. For example, we want to obtain a composite with maximum damping or maximum stiffness along direction 1 for a 2D composite. The optimization problem can be defined as

$$\begin{aligned} &\text{Maximize: } f(x_e) = \tan\delta_{1111}(\omega) \quad \text{or} \quad E'_{1111}(\omega) \\ &\text{Subject to: } V_f^{1*} = \sum_{e=1}^{N} V_e x_e \Big/ \sum_{e=1}^{N} V_e \end{aligned} \tag{12}$$

where $f(x_e)$ is the objective function. V_e is the volume of the eth element and V_f^{1*} is the prescribed volume fraction of material 1 which can be specified by the user. N is the total number of elements in the unit cell. It should be noted that the numerical examples in this paper will consider maximizing damping and/or stiffness in both directions (1 and 2). Certainly, other optimization problems with damping and stiffness properties of composites can also be formulated and equally solved by the proposed BESO algorithm in this paper.

3.3. Sensitivity analysis

To implement the BESO optimization technique, sensitivity analysis is necessary for guiding the search direction during the iteration process. As the given objective functions in Eq. (12) can be calculated from the modulus matrix, it is necessary to compute the sensitivity of the complex modulus with regard to design variables. With the help of the material interpolation scheme in Eqs. (10) and (11), the derivation of the complex modulus E^H_{ijkl} with respect to design variables x_e can be easily obtained by using the adjoint method [31,33,43].

$$\frac{\partial E^H_{ijkl}}{\partial x_e} = \frac{1}{|Y|}\int_{\Omega_e}\left[p x_e^{p-1}(E'^{(1)}_{ijpq} - E'^{(2)}_{ijpq}) + i(E''^{(1)}_{ijpq} - E''^{(2)}_{ijpq})\right](\bar{\varepsilon}^{kl}_{pq} - \tilde{\varepsilon}^{kl}_{pq})d\Omega_e \tag{13}$$

where Ω_e is the domain of the eth element. It can be seen that the resulting sensitivity is also complex where the real part is the sensitivity of storage modulus and the imaginary part is the sensitivity of loss modulus. Here, the detailed derivations for sensitivity analysis are overlooked and the reader may refer to Refs. [31,33]. In the proposed BESO method, the design variables x_e are restricted to be binary values either 0 or 1, thus the elemental sensitivity can be expressed explicitly as

$$\frac{\partial E^H_{ijkl}}{\partial x_e} = \begin{cases} \dfrac{1}{|Y|}\displaystyle\int_{\Omega_e}\left[(E'^{(1)}_{ijpq} - E'^{(2)}_{ijpq}) + i(E''^{(1)}_{ijpq} - E''^{(2)}_{ijpq})\right](\bar{\varepsilon}^{kl}_{pq} - \tilde{\varepsilon}^{kl}_{pq})d\Omega_e & \text{when } x_e = 1 \\ \dfrac{1}{|Y|}\displaystyle\int_{\Omega_e}\left[i(E''^{(1)}_{ijpq} - E''^{(2)}_{ijpq})\right](\bar{\varepsilon}^{kl}_{pq} - \tilde{\varepsilon}^{kl}_{pq})d\Omega_e & \text{when } x_e = 0. \end{cases} \tag{14}$$

3.4. Numerical implementation

The BESO method [41] normally used sensitivity numbers to update the design variable x_e where sensitivity numbers denote the relative ranking of elemental sensitivities. For the maximization optimization problem, elemental sensitivity number for the eth element can be simply expressed by

$$\alpha_e = \frac{\partial f(x_e)}{\partial x_e}. \tag{15}$$

As the objective function is composed of the combination of the components of E^H_{ijkl}, the elemental sensitivity numbers can be easily obtained by substituting Eq. (14) into Eq. (15). According to the relative ranking of elemental sensitivity numbers, BESO will update the design variables $x_e = 0$ for elements with the lowest sensitivity numbers and $x_e = 1$ for elements with highest sensitivity numbers.

Numerical instabilities such as checkerboard pattern and mesh-dependency problem are common phenomenon in the topology optimization techniques based on the finite element analysis [44]. Here, a mesh-independent filter for

Table 1
The properties of materials 1 and 2 at the operation frequencies.

	Operation frequency ω (rad/s)	Storage modulus E'_{1111} (GPa)	Loss modulus E''_{1111} (GPa)	Loss tangent	Bulk modulus κ (GPa)
Material 1	All	73.56	0.00	0.00	44.87
Material 2	0	1	0.00	0.00	0.77
	0.5	1.71	1.14	0.67	$1.32 + 0.88i$

discrete design variables [14] is applied for the sensitivity numbers. The modified elemental sensitivity number can be expressed by

$$\hat{\alpha}_i = \frac{\sum_{j=1}^{N} w(r_{ij})\alpha_j}{\sum_{j=1}^{N} w(r_{ij})} \tag{16}$$

where r_{ij} denotes the distance between the centers of elements i and j. $w(r_{ij})$ is the weight factor of the jth sensitivity number as

$$w(r_{ij}) = \begin{cases} r_{\min} - r_{ij} & \text{for } r_{ij} < r_{\min} \\ 0 \quad \text{for } r_{ij} \geq r_{\min} \end{cases} \tag{17}$$

where $r_{\min}$ is the filter radius which can be specified by the user.

Due to the discrete design variables used in the BESO algorithm, Huang and Xie [14] proposed that the sensitivity number can be further modified by averaging with its historical information to improve the convergence of the solution. Thus, the sensitivity number after the first iteration can be further modified by

$$\tilde{\alpha}_{i,k} = \frac{1}{2}\left(\hat{\alpha}_{i,k} + \tilde{\alpha}_{i,k-1}\right) \tag{18}$$

where k is the current iteration number.

BESO starts from an initial design and update the topology of the unit cell according to the calculated sensitivity numbers step by step. The whole iteration process is stopped until both the volume fraction constraint is satisfied and the objective function is convergent. For the detailed BESO procedure one can also refer to Refs. [15,19,23].

4. Numerical examples and discussions

Some numerical examples are presented in this section to illustrate the microstructural design of viscoelastic composites and demonstrate the effectiveness of the proposed optimization approach. It is assumed that the viscoelastic composite is composed of two materials: one is pure elastic and another is viscoelastic. Both materials are assumed to be isotropic and their material properties are Young's modulus $E^{(1)} = 70$ GPa, Poisson's ratio $v^{(1)} = 0.22$ for material 1 (glass) and $E^{(2)} = 1 + 2.5e^{-t}$ GPa, $v^{(2)} = 0.35$ for material 2 (epoxy). The storage and loss moduli, loss tangent and bulk modulus for both materials at the frequencies $\omega = 0$ and 0.5 rad/s are listed in Table 1. However, it should be noted that the proposed optimization algorithm can be equally applied for two viscoelastic materials.

The unit cell which represents the microstructure of a composite is discretized with 80×80 square bilinear finite elements. To initialize the optimization process, the initial guess is assumed to be that the unit cell is full of material 1 except for four elements at the center of the unit cell with material 2. The evolution rate $ER = 2\%$ and $r_{\min}$ is selected to be 5 times of the typical size of elements. In the following figures of the unit cells, black elements represent material 1 (stiff and elastic) and white elements represent material 2 (soft and viscoelastic).

4.1. Examples for maximizing damping of composites

The high damping at the operation frequency is mostly desirable for the design of viscoelastic materials. The objective of numerical examples in this section is to find microstructures so that the resulting composites yield damping

Table 2
Optimized results for maximizing damping of composites.

V_f^1	Unit cell	4×4 unit cells	Elasticity matrix (GPa)	$\delta_{1111}(=\delta_{2222})$
80%	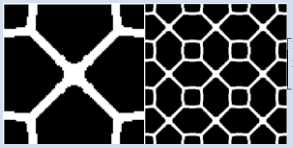		$\begin{bmatrix} 11.8+6.26i & 3.58+1.83i & 0 \\ 3.58+1.83i & 11.8+6.26i & 0 \\ 0 & 0 & 4.76+2.45i \end{bmatrix}$	0.53
70%	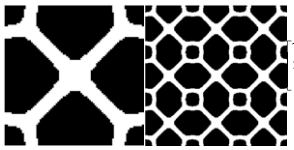		$\begin{bmatrix} 7.57+4.40i & 2.55+1.44i & 0 \\ 2.55+1.44i & 7.57+4.40i & 0 \\ 0 & 0 & 3.19+1.79i \end{bmatrix}$	0.58
60%			$\begin{bmatrix} 5.11+3.14i & 2.18+1.28i & 0 \\ 2.18+1.28i & 5.11+3.14i & 0 \\ 0 & 0 & 2.67+1.54i \end{bmatrix}$	0.61
50%			$\begin{bmatrix} 4.02+2.53i & 1.65+1.01i & 0 \\ 1.65+1.01i & 4.02+2.53i & 0 \\ 0 & 0 & 1.88+1.14i \end{bmatrix}$	0.63
40%			$\begin{bmatrix} 3.27+2.10i & 1.29+0.81i & 0 \\ 1.29+0.81i & 3.27+2.10i & 0 \\ 0 & 0 & 1.38+0.86i \end{bmatrix}$	0.64

along directions 1 and 2 at $\omega = 0.5$ rad/s as large as possible. The optimization objective is defined as

$$\text{maximize: } f = \tan\delta_{1111}(\omega) + \tan\delta_{2222}(\omega) \quad \text{at } \omega = 0.5 \text{ rad/s}. \tag{19}$$

The proposed BESO method was applied for the above optimization problem under various given volume fractions of material 1. Table 2 lists the resulting microstructures of optimized composites and their properties. The optimized microstructures show that the stiff and elastic material 1 is surrounded by soft and viscoelastic material 2 so as to maximize the damping of the resulting composites. It is interesting to note that the material damping is significantly enhanced by adding a small amount of the viscoelastic material into the elastic material without any damping. For instance, the loss tangent $\delta_{1111} = \delta_{2222} = 0.53$ when $V_f^1 = 0.8$. Further increasing the volume fraction of the viscoelastic material only causes the insignificant increase of the loss tangent. When $V_f^1 = 0.4$, the loss tangent $\delta_{1111} = \delta_{2222} = 0.64$ which is very close to that of the pure viscoelastic material 2, $\delta_{1111} = \delta_{2222} = 0.67$. Nevertheless, the microstructures with disconnected stiff material 1 as shown in Table 2 inevitably lead to composites with low stiffness (storage modulus) because maximizing material damping is equivalent to maximizing loss modulus and minimizing storage modulus simultaneously (the loss tangent is the ratio of the loss modulus to the storage modulus). Fig. 2 gives the changes of damping, storage modulus and loss modulus with the variation of the volume fraction of material 1. It can be seen that the material damping decreases as the volume fraction of material 1 increases and it becomes zero when the microstructure is full of material 1. Both the storage modulus and loss modulus increase with the increase of volume fraction of material 1, but the loss modulus finally returns to zero when $V_f^1 = 100\%$. The maximum value of loss modulus in Fig. 2 corresponds to that for $V_f^1 = 90\%$ because we only conducted limited cases for the given volume fraction constraints. However, it should note that the actual maximum loss modulus should occur at some volume fraction $90\% < V_f^1 < 100\%$. This maximum loss modulus is less important with regard to the material design because the corresponding composite must be with low damping as shown in Fig. 2.

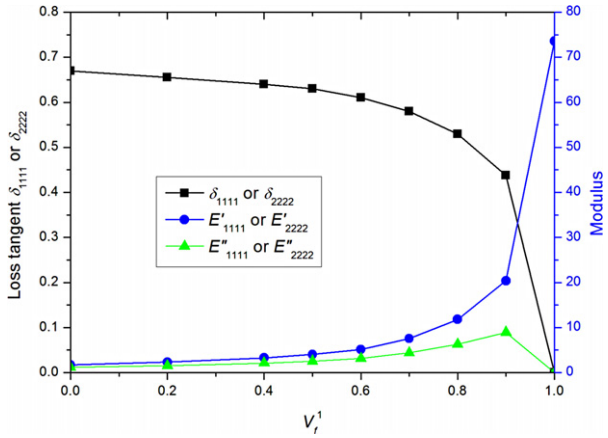

Fig. 2. Variations of loss tangent, storage and loss moduli for maximizing damping under various volume fraction constraints.

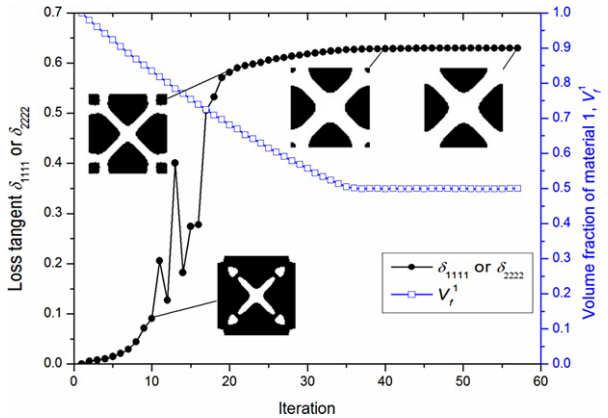

Fig. 3. Evolution histories of loss tangent, volume fraction and topology for maximizing damping with the volume fraction $V_1^f = 50\%$.

Fig. 3 plots the evolution histories of the objective function and volume fraction of material 1 when the objective volume fraction of material 1 is set to be 50%. BESO starts from the initial design being almost full of material 1, gradually decreases the volume fraction of material 1 to its prescribed value 50% and then keeps constant. The composite damping is generally improved as more and more viscoelastic material 2 is added to the unit cell. At the latest stage of the optimization, both the composite damping and microstructure are stably convergent to the solutions while the volume fraction of material 1 keeps its constraint value 50%.

4.2. *Examples for maximizing stiffness of composites*

Apart from the viscoelastic damping, the material stiffness (storage modulus) also has the significant effect on the reduction of vibration and noise. The optimization objective of numerical examples in this section is to maximizing the storage modulus of composites along both directions 1 and 2 at the operation frequency $\omega = 0.5$ rad/s. Thus, the optimization objective is expressed by

$$\text{maximize: } f = E_{1111}(\omega) + E_{2222}(\omega) \quad \text{at } \omega = 0.5 \text{ rad/s}. \tag{20}$$

Table 3 gives the optimized microstructures of composites and their material properties under various volume fractions of material 1. Totally different from the optimized microstructures for maximizing damping in Section 4.1, maximizing stiffness of composites always leads to the optimized microstructures with connected stiff and elastic material 1. Fig. 4 shows the variations of the resulting loss tangent, storage modulus and loss modulus against the volume fraction of material 1. It can be seen that the loss modulus always keeps at a very low level (less than 1.16)

Table 3
Optimized results for maximizing stiffness of composites.

V_f^1	Unit cell	4×4 unit cells	Elasticity matrix (GPa)	$\delta_{1111}(=\delta_{2222})$
80%	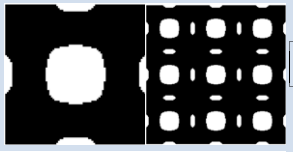		$\begin{bmatrix} 46.81+0.84i & 9.12+0.35i & 0 \\ 9.12+0.35i & 46.81+0.84i & 0 \\ 0 & 0 & 11.43+0.72i \end{bmatrix}$	0.018
60%	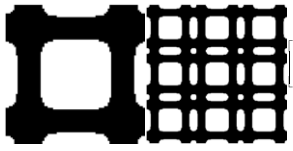		$\begin{bmatrix} 30.32+1.08i & 4.66+0.45i & 0 \\ 4.66+0.45i & 30.32+1.08i & 0 \\ 0 & 0 & 3.61+0.78i \end{bmatrix}$	0.036
50%	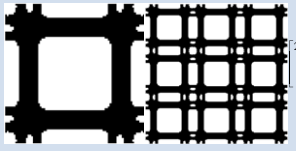		$\begin{bmatrix} 23.98+1.14i & 3.06+0.47i & 0 \\ 3.06+0.47i & 23.98+1.14i & 0 \\ 0 & 0 & 0.15+0.69i \end{bmatrix}$	0.047
30%	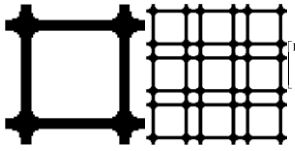		$\begin{bmatrix} 13.58+1.16i & 1.47+0.45i & 0 \\ 1.47+0.45i & 13.58+1.16i & 0 \\ 0 & 0 & 1.00+0.54i \end{bmatrix}$	0.085
20%	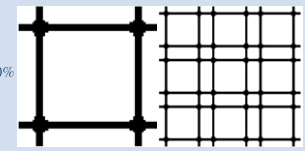		$\begin{bmatrix} 9.29+1.16i & 0.99+0.44i & 0 \\ 0.99+0.44i & 9.29+1.16i & 0 \\ 0 & 0 & 0.77+0.47i \end{bmatrix}$	0.125

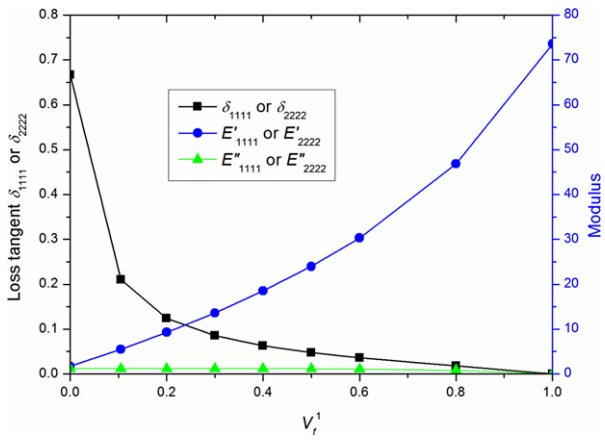

Fig. 4. Variations of loss tangent, storage and loss moduli for maximizing stiffness under various volume fraction constraints.

for all cases. As the result, the loss tangent quickly decreases to a low level even if a small amount of elastic material 1 adds to the viscoelastic material 2, e.g. $\delta_{1111} = \delta_{2222} = 0.125$ for $V_1^f = 20\%$.

4.3. Comparison with bounds of effective bulk moduli

To further check the optimized solutions, the obtained results can be compared with the theoretical bounds of effective bulk moduli. Unfortunately, the theoretical bounds for viscoelastic composites cannot be easily expressed by

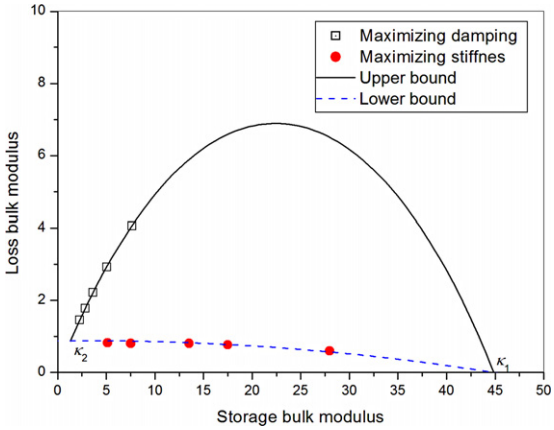

Fig. 5. Bounds of effective bulk modulus in the complex plane.

explicit formulae. Gibiansky and Lakes [29,30] investigated the set of possible values of the complex effective bulk modulus κ should fill a region in the complex plane because κ is described by two numbers, i.e. its real and imaginary parts. At the operation frequency $\omega = 0.5$ rad/s, bounds of the effective bulk modulus in the complex plane can be obtained numerically as shown in Fig. 5 where the solid and dash lines denote the upper and lower bounds of loss bulk modulus respectively. In Fig. 5, the hollow squares denote the effective bulk moduli for the composites with maximum damping given in Table 2, and solid circles denote the effective bulk moduli of the composites with maximum stiffness given in Table 3. It clearly shows that the effective bulk moduli for maximizing damping are coincident with the upper bound of loss bulk modulus, however the effective bulk moduli for maximizing stiffness is located at the lower bound of loss bulk modulus. As discussed in Section 4.1, the loss bulk modulus can be further increased by increasing the volume fraction of material 1. According to the theoretical upper bound of the loss bulk modulus, the maximum loss bulk modulus is about 6.9 GPa and the corresponding storage bulk modulus and loss tangent are about 22.6 GPa and 0.3 respectively.

The bounds for the storage modulus against volume fraction can be described by Hashin–Shtrikman (H–S) bounds through the replacement of elastic moduli with corresponding viscoelastic complex moduli [27,28]. The numerical H–S upper and lower bounds of the storage bulk modulus are plotted in Fig. 6. The storage bulk moduli of the optimized composites in Tables 2 and 3 are given in Fig. 6 with hollow squares and solid circles. It can be seen that the storage bulk moduli of the optimized composites for maximizing stiffness approach the H–S upper bound, and the storage bulk moduli of the optimized composites for maximizing damping are very close to the H–S lower bound.

4.4. Examples for maximizing damping with stiffness constraint

Examples in the above sections indicate that maximizing damping and stiffness are somewhat conflicting optimization objectives for the design of viscoelastic composites and the design of viscoelastic composites is therefore an inherent multi-objective optimization problem. The possible ranges of damping and stiffness of composites under a given volume fraction can be estimated by previous examples as they approach the theoretical bounds of storage and loss moduli, for instance, $0.047 \leq \delta_{1111}\,(=\delta_{2222}) \leq 0.63$ and $4.02\ \text{GPa} \leqslant E'_{1111}\left(=E'_{2222}\right) \leqslant 23.98\ \text{GPa}$ when $V_f^1 = 50\%$. With the above limits in mind, we will maximize composite damping by setting a series of stiffness constraints in this section. To this end, the optimization problem can be stated as

$$\begin{aligned}
&\text{maximize: } f = \tan\delta_{1111}(\omega) + \tan\delta_{2222}(\omega) \quad \text{at } \omega = 0.5\\
&\text{subject to: } E'_{1111}(\omega)\left(=E'_{2222}(\omega)\right) = E^* \quad \text{at } \omega = 0.5\\
&V_f^{1*} = \sum_{e=1}^{N} V_e x_e \Big/ \sum_{e=1}^{N} V_e = 50\%
\end{aligned} \tag{21}$$

here, E^* is the constraint value of the storage modulus in directions 1 and 2. Such an additional constraint on the storage modulus can be easily satisfied by introducing a Lagrange multiplier as given in Ref. [45].

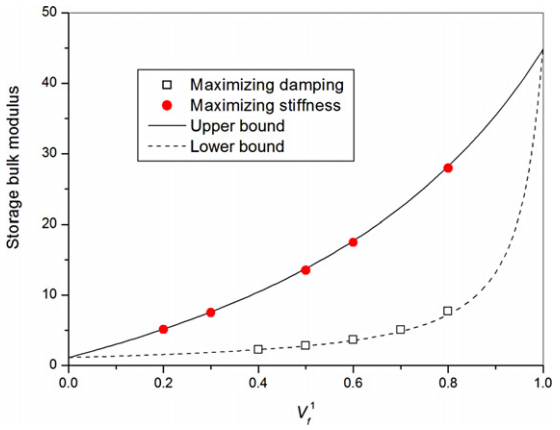

Fig. 6. Bounds of storage bulk modulus under various volume fractions.

Table 4
Optimized results for maximizing damping with stiffness constraint.

E^*	Unit cell	4×4 unit cells	Elasticity matrix (GPa)	$\delta_{1111}(=\delta_{2222})$
5			$\begin{bmatrix} 4.97+2.97i & 1.98+1.12i & 0 \\ 1.98+1.12i & 4.97+2.97i & 0 \\ 0 & 0 & 1.63+1.00i \end{bmatrix}$	0.60
10	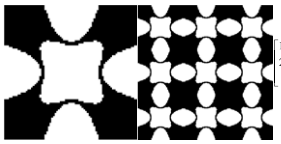		$\begin{bmatrix} 10.0+3.02i & 2.28+0.97i & 0 \\ 2.28+0.97i & 10.0+3.02i & 0 \\ 0 & 0 & 1.61+0.87i \end{bmatrix}$	0.30
15			$\begin{bmatrix} 15.1+1.80i & 5.07+0.58i & 0 \\ 5.07+0.58i & 15.1+1.80i & 0 \\ 0 & 0 & 5.87+0.59i \end{bmatrix}$	0.12
20	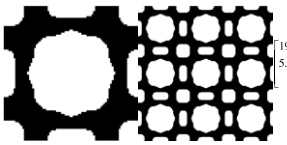		$\begin{bmatrix} 19.9+1.60i & 5.62+0.14i & 0 \\ 5.62+0.14i & 19.9+1.60i & 0 \\ 0 & 0 & 3.05+0.72i \end{bmatrix}$	0.08

The optimized microstructures and their material properties are given in Table 4 for $E^* = 5$ GPa, 10 GPa, 15 GPa, and 20 GPa respectively. It can be seen that the stiff and elastic material 1 in the optimized microstructures is disconnected for $E^* = 5$ GPa, weakly connected for $E^* = 10$ GPa and strongly connected for $E^* = 15$ GPa and 20 GPa. Meanwhile, the loss tangent decreases from 0.6 for $E^* = 5$ GPa to 0.08 for $E^* = 20$ GPa. The elasticity matrixes in Table 4 shows the resulting storage moduli are very close to the corresponding constraint values.

As mentioned above, the design of viscoelastic composite is in fact of a multi-objective optimization problem which maximizes damping and stiffness simultaneously. To conveniently plot the Pareto front curve for this multi-objective optimization problem, the damping and stiffness are inversely non-dimensionalized by their minimum values $\delta_{\min} = 0.047$ and $E_{\min} = 4.02$ GPa so that $0 < \delta_{\min}/\delta \leq 1$ and $0 < E_{\min}/E' \leq 1$. The plotting of non-dimensional damping against stiffness gives the Pareto front with a convex curve as shown in Fig. 7. The right above the Pareto front curve gives the region for possible designs but the optimal solution should be on the Pareto front. The optimal

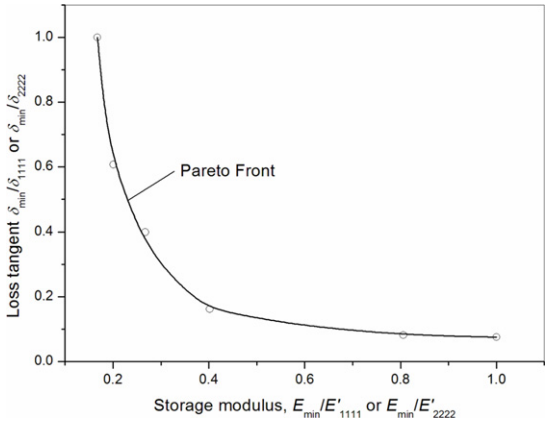

Fig. 7. Relationship between loss tangent and storage modulus of optimized viscoelastic composites.

Table 5
Optimized results for maximizing damping with stiffness constraint under different operation frequencies.

E^* at $\omega=0$	Unit cell	4×4 unit cells	Elasticity matrix at $\omega=0.5$	$\delta_{1111}(=\delta_{2222})$ at $\omega=0.5$
5		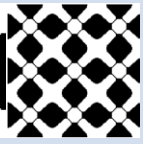	$\begin{bmatrix} 8.86+2.64i & 3.91+0.85i & 0 \\ 3.91+0.85i & 8.86+2.64i & 0 \\ 0 & 0 & 2.63+1.38i \end{bmatrix}$	0.38
10		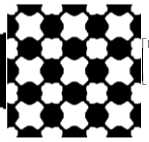	$\begin{bmatrix} 11.70+2.14i & 7.08+0.49i & 0 \\ 7.08+0.49i & 11.70+2.14i & 0 \\ 0 & 0 & 5.88+1.22i \end{bmatrix}$	0.18
15			$\begin{bmatrix} 16.31+1.95i & 5.21+0.59i & 0 \\ 5.21+0.59i & 16.31+1.95i & 0 \\ 0 & 0 & 5.23+0.78i \end{bmatrix}$	0.12
20		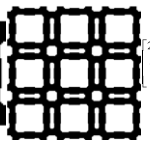	$\begin{bmatrix} 21.20+1.59i & 4.96+0.35i & 0 \\ 4.96+0.35i & 21.20+1.59i & 0 \\ 0 & 0 & 3.31+0.89i \end{bmatrix}$	0.075

design of viscoelastic composite is therefore a matter of making a trade-off decision from a set of compromising solutions on the Pareto front.

In some cases, viscoelastic material is required with high stiffness at a low frequency and high damping at a high frequency. Thus, the optimization problem can be reformulated e.g. to maximize the damping at the high frequency $\omega = 0.5$ rad/s subject to the static stiffness constraint.

$$\begin{aligned} &\text{maximize: } f = \tan\delta_{1111}(\omega) + \tan\delta_{2222}(\omega) \quad \text{at } \omega = 0.5 \text{ rad/s} \\ &\text{subject to: } E'_{1111}(\omega)\left(= E'_{2222}(\omega)\right) = E^* \quad \text{at } \omega = 0 \\ &V_f^{1*} = \sum_{e=1}^{N} V_e x_e \Big/ \sum_{e=1}^{N} V_e = 50\%. \end{aligned} \tag{22}$$

The proposed BESO method can also be applied for this optimization problem except for the homogenization calculation for both frequencies which inevitably causes high computational cost. The resulting microstructures of composites, elasticity matrixes and loss tangent are given in Table 5 when the static stiffness constraint is set to be $E^* = 5$ GPa, 10 GPa, 15 GPa, and 20 GPa respectively. The optimized microstructures are obviously different from those in Table 4 and demonstrate that the design of composites depends on the application requirements.

5. Conclusions

In this paper, viscoelastic composites are supposed to be composed of a stiff and elastic material phase and a soft and viscoelastic material. The BESO method is extended to designing microstructures of composites with desirable viscoelastic properties. The given examples demonstrate the effectiveness of the proposed optimization algorithm to obtain the clear microstructures of composites with maximum damping and/or stiffness. The numerical results indicate that the damping property of composites can be greatly enhanced by properly mixing a small amount of a viscoelastic material with an elastic material, but stiffness of composites has no significant improvement. When the optimization objective changes to maximize the stiffness of composites, the damping property of viscoelastic material phase cannot be fully utilized. Comparison with theoretical bounds reveal that maximizing damping results in designs at the upper bound of loss modulus and the lower bound of storage modulus, but maximizing stiffness results in designs at the lower bound of loss modulus and the upper bound of storage modulus. Therefore, the design of viscoelastic composites is inherently a multi-objective optimization problem which is solved by maximizing damping subject to a stiffness constraint in this paper. A set of Pareto optimal solutions is obtained in the presence of trade-offs between conflicting damping and stiffness objectives for the design of viscoelastic composites.

Acknowledgment

The authors wish to acknowledge the financial support from the Australian Research Council (FT130101094) and Key Program of National Natural Science Foundation of China (61232014) for carry out this work.

References

[1] D.D.L. Chung, Review materials for vibration damping, J. Mater. Sci. 36 (2001) 5733–5737.
[2] R.M. Christensen, Theory of Viscoelasticity, Dover, New York, 2010.
[3] R.S. Lake, High damping composite materials: effect of structural hierarchy, J. Compos. Mater. 36 (3) (2002) 287–297.
[4] M.P. Bendsøe, N. Kikuchi, Generating optimal topologies in structural design using a homogenization method, Comput. Methods Appl. Mech. Engrg. 71 (1988) 197–224.
[5] M.P. Bendsøe, Optimal shape design as a material distribution problem, Struct. Optim. 1 (1989) 193–202.
[6] G.I.N. Rozvany, M. Zhou, T. Birker, Generalized shape optimization without homogenization, Struct. Optim. 4 (1992) 250–254.
[7] M. Zhou, G.I.N. Rozvany, The COC algorithm, part II: topological, geometry and generalized shape optimization, Comput. Methods Appl. Mech. Engrg. 89 (1991) 197–224.
[8] M.P. Bendsøe, O. Sigmund, Topology Optimization: Theory, Methods and Applications, Springer-Verlag, Berlin, 2003.
[9] M.Y. Wang, X. Wang, D. Guo, A level set method for structural topology optimization, Comput. Methods Appl. Mech. Engrg. 192 (2003) 227–246.
[10] X. Wang, M.Y. Wang, D. Guo, Structural shape and topology optimization in a level-set-based framework of region representation, Struct. Multidiscip. Optim. 27 (2004) 1–19.
[11] J.A. Sethian, A. Wiegmann, Structrual boundary design via level set and immersed interface methods, J. Comput. Phys. 163 (2) (2000) 489–528.
[12] Y.M. Xie, G.P. Steven, A simple evolutionary procedure for structural optimization, Comput. Struct. 49 (1993) 885–896.
[13] Y.M. Xie, G.P. Steven, Evolutionary Structural Optimization, Springer, London, 1997.
[14] X. Huang, Y.M. Xie, Convergent and mesh-independent solutions for the bi-directional evolutionary structural optimization method, Finite Elem. Anal. Des. 43 (14) (2007) 1039–1049.
[15] X. Huang, Y.M. Xie, Evolutionary Topology Optimization of Continuum Structures: Methods and Applications, John Wiley & Sons, Chichester, 2010.
[16] O. Sigmund, Materials with prescribed constitutive parameters: an inverse homogenization problem, Internat. J. Solids Structures 31 (1994) 2313–2329.
[17] O. Sigmund, Tailoring materials with prescribed elastic properties, Mech. Mater. 20 (1995) 351–368.
[18] M.M. Neves, H. Rodrigues, J.M. Guedes, Optimal design of periodic linear elastic microstructures, Comput. Struct. 20 (2000) 421–429.
[19] X. Huang, A. Radman, Y.M. Xie, Topological design of microstructures of cellular materials for maximum bulk or shear modulus, Comput. Mater. Sci. 50 (2011) 1861–1870.

[20] S.W. Zhou, Q. Li, Computational design of multi-phase microstructural materials for extremal conductivity, Comput. Mater. Sci. 43 (2008) 549–564.
[21] J.K. Guest, J.H. Prevost, Design of maximum permeability material structures, Comput. Methods Appl. Mech. Engrg. 196 (4–6) (2007) 1006–1017.
[22] S.W. Zhou, W. Li, G. Sun, Q. Li, A level-set procedure for the design of electromagnetic metamaterials, Opt. Express 18 (7) (2010) 6693–6702.
[23] X. Huang, Y.M. Xie, B. Jia, Q. Li, S.W. Zhou, Evolutionary topology optimization of peridodic composites for extremal magnetic permeability and electrical permittivity, Struct. Multidiscip. Optim. 46 (2010) 385–398.
[24] S. Torquato, S. Hyun, A. Donev, Multifunctional composites: optimizing microstructures for simultaneous transport of heat and electricity, Phys. Rev. Lett. 89 (2002) 266601.
[25] J.K. Guest, J.H. Prevost, Optimizing multifunctional materials: design of microstructures for maximized stiffness and fluid permeability, Internat. J. Solids Structures 43 (22–23) (2006) 7028–7047.
[26] V.J. Challis, A.P. Roberts, A.H. Wilkins, Design of three dimensional isotropic microstructures for maximized stiffness and conductivity, Internat. J. Solids Structures 45 (2008) 4130–4146.
[27] Z. Hashin, S. Shtrikman, A variational approach to the theory of the elastic behaviour of multiphase materials, J. Mech. Phys. Solids 11 (2) (1963) 127–140.
[28] Z. Hashin, Complex moduli of an viscoelastic composites: I General theory and application to particulate composites, Internat. J. Solids Structures 6 (1965) 539–552.
[29] L.V. Gibiansky, G.W. Milton, On the effective viscoelastic moduli of two-phase media: I. Rigorous bounds on the complex bulk modulus, Proc. R. Soc. Lond. A 440 (1993) 163–188.
[30] L.V. Gibiansky, R. Lakes, Bounds on the complex bulk modulus of a two-phase viscoelastic composite with arbitrary volume fractions of the components, Mech. Mater. 16 (1993) 317–331.
[31] Y.-M. Yi, S.-H. Park, S.-K. Youn, Design of microstructrues of viscoelastic composites for optimal damping characteristics, Internat. J. Solids Structures 37 (2000) 4791–4810.
[32] J. Prasad, A.R. Diaz, Viscoelastic material design with negative stiffness components using topology optimization, Struct. Multidiscip. Optim. 38 (2009) 583–597.
[33] W. Chen, S. Liu, Topology optimization of microstructures of viscoelastic damping materials for a prescribed shear modulus, Struct. Multidiscip. Optim. (2014) http://dx.doi.org/10.1007/s00158-014-1049-3. online.
[34] C.S. Andreasen, E. Andreassen, J.S. Jensen, O. Sigmund, On the realization of the bulk modulus bounds for two-phase viscoelastic composites, J. Mech. Phys. Solids 63 (2014) 228–241.
[35] E. Andreassen, J.S. Jesen, Topology optimization of periodic microstructures for enhanced dynamic properties of viscoelastic composite materials, Struct. Multidiscip. Optim. 49 (2014) 695–705.
[36] X. Huang, S.W. Zhou, Y.M. Xie, Q. Li, Topology optimization of microstructures of cellular materials and composites for macrostructures, Comput. Mater. Sci. 67 (2013) 397–407.
[37] L. Xia, P. Breitkopf, Concurrent topology optimization design of material and structure within FE2 nonlinear multiscale analysis framework, Comput. Methods Appl. Mech. Engrg. 278 (2014) 524–542.
[38] Y.-M. Yi, S.-H. Park, S.-K. Youn, Asympotic homogenization of viscoelastic composites with periodic microstructures, Internat. J. Solids Structures 35 (1998) 2039–2055.
[39] B. Hassani, E. Hinton, A review of homogenization and topology optimization I—homogenization theory for media with periodic structure, Comput. Struct. 69 (1998) 707–717.
[40] B. Hassani, E. Hinton, A review of homogenization and topology optimization II—analytical and numerical solution of homogenization equations, Comput. Struct. 69 (1998) 719–738.
[41] X. Huang, Y.M. Xie, Bi-directional evolutionary topology optimization of continuum structures with one or multiple materials, Comput. Mech. 43 (3) (2009) 393–401.
[42] X. Huang, Y.M. Xie, A further review of ESO type methods for topology optimization, Struct. Multidiscip. Optim. 41 (2010) 671–683.
[43] E.J. Haug, K.K. Choi, V. Komkov, Design Sensitivity Analysis of Structural Systems, Academic Press, Orlando, 1986.
[44] O. Sigmund, J. Petersson, Numerical instabilities in topology optimization: a survey on procedures dealing with checkerboards, mesh-dependencies and local minima, Struct. Optim. 16 (1) (1998) 68–75.
[45] X. Huang, Y.M. Xie, Evolutionary topology optimization of continuum structures with an additional displacement constraint, Struct. Multidiscip. Optim. 40 (2012) 409–416.